DOI 10.1007/s11595-016-1487-4

Influence of Curing Duration on Thaumasite Formation of Portland-limestone Cement Pastes

LOU Liangwei[1,2]

(1.Railway Engineering Research Institute, China Academy of Railway Sciences, Beijing 100081, China; 2.State Key Laboratory for Track Technology of High−Speed Railway, Beijing 100081, China)

Abstract: Extensive researches have been carried out on the conventional sulfate attack, while it has been found that the thaumasite form of sulfate attack (TSA), sulfate attack at low temperature, has just been discovered and its mechanism is not well understood so far. In this study, the sulfate attack of cement paste incorporating 30% mass of limestone powder was investigated. After 20 ℃ water cured for 7, 14, and 28 days, respectively, 20 mm cube specimens were exposed in a 5% magnesium sulfate solution at (6 ±1) ℃ for periods up to 240 days. Their appearance change, compressive strength development were examined at different storage time, and selected paste samples were examined by X-ray diffraction (XRD), Fourier transform infrared spectroscopy (FTIR), scanning electron microscopy (SEM) and energy dispersive spectroscopy (EDS). The results indicate that all Portland-limstone cement pastes suffer from appearance deterioration to some extent. The compressive strength of cement paste initially increases and after 120 days decreases with increasing exposed period. In addition, the cement paste with short curing time is more susceptible to sulfate attack, which directly leads to the formation of non-binder thaumasite crystal accompanied by the formation of ettringite, gypsum and brucite, and becomes a white, mushy, and incohesive matrix. Additionally, the extent of sulfate attack is greater and the formation of thaumasite is observed earlier for shorter curing time.

Key words: thaumasite; sulfate attack; limestone; curing; low temperature

1 Introduction

Conventional sulfate attack can be defined as a physico-chemical reaction, leading to an expansion stress due to ettringite and gypsum formation, which results in the loss of strength because of destabilizing calcium silicate hydrate (C-S-H) gel. Unlike the general form of sulfate attack, the formation of thaumasite ($CaSiO_3 \cdot CaCO_3 \cdot CaSO_4 \cdot 15H_2O$) directly causes deterioration associated with the conversion of C-S-H into an incohesive mass by an unnoticeable reaction[1]. The main differences between TSA and conventional sulfate attack are low temperature and limestone presence that have been highlighted in previous works[2-4].

Erlin and Stark first determined thaumasite attack in cement and concrete and investigated the products of deterioration in 1965[5]. Over decades, other instances regarding this formation of sulfate attack have also been reported widely[6-8]. In particular, curing has proven to be a crucial parameter in improving TSA-resistance of test concretes made using either Portland cement or sulfate resistant Portland cement and limestone aggregate[9]. And an initial air curing was found to be very beneficial as already noted[10]. Therefore, the main objective of the investigation presented in this study is to investigate the effect of curing regimes on thaumasite formation. Cement-limestone based pastes subjected to magnesium sulfate solution at specific temperatures were examined using visual inspection, mechanical test and mineralogy analysis.

2 Experimental

2.1 Materials

Cement clinker with added 4% dihydrate gypsum was ground for 45 minutes in a ball mill, and the specific surface area of cement particles is around

(Received: Dec. 20, 2015; Accepted: June 8, 2016)

LOU Liangwei(楼梁伟): Research Assistant; E-mail: louliangwei@163.com

Funded by National Natural Science Foundation of China (No. 51378499), China Railway Corporation (No. 2014G004-R), Science and Technology of China (No. 2010G004-E)

360 m^2/kg with a density of 3.0 g/cm^3. Moreover, the limestone was ground to a specific surface area of 420 m^2/kg. The chemical compositions of cement and ground limestone are given in Table 1, and the basic properties of cement were measured and are reported in Table 2.

Table 1 Compositions of cement and ground limestone/wt%

Materials	CaO	SiO_2	Al_2O_3	Fe_2O_3	MgO	SO_3	Na_2O	Loss
Cement	63.67	21.40	5.63	3.65	2.15	1.75	1.02	0.73
Limestone	54.37	0.19	-	0.39	0.57	-	0.09	42.05

2.2 Sample preparation

In total, 21 groups of cement paste cube specimens, 20 mm×20 mm×20 mm, were manufactured and the water to binder (cement incorporating limestone) ratio was 0.30. The limestone powder replaced cement at the level of 30% by mass. The tested specimens named JY-1, JY-2, and JY-3 represent water cured for 7, 14 and 28 days after demoulding. After curing, the specimens were submerged in 5.0% magnesium sulfate solution and were placed in the temperature controlled chamber (6 ±1 ℃). The specimens and solution were kept in sealed containers with a solution to specimens volume ratio of 1.5:1, and the solution was changed every two months.

2.3 Test methods

All specimens were visually examined to identify the physical changes of the exposed surface and the formation of reaction products was carefully recorded by a digital camera. The compressive strength of cement paste was tested at different storage age up to 240 days in order to investigate the influence of the thaumasite sulfate attack on the strength of the samples.

Microstructures of the cement paste samples were studied using scanning electron microscope (SEM) together with energy dispersive spectrometer (EDS) analysis. A VEGA Ⅱ LMU scanning electron microscope machine from Tescan Ltd was used with the resolution of 3.0 nm/30 kV under high vacuum mode (SE) and 3.5 nm/30 kV under low vacuum mode (BSE, LVSTD). Its magnification was between 4 times and 100 000 times with acceleration voltage of 0.2-30 kV and a beam current of 1 pA-2 uA. Prior to investigation, the 5 mm cube samples were dried to constant weight in the desiccators after suspending hydration for 48 hours, and the gold coating was applied.

In order to identify the compounds formed during the storage in the sulfate solution, X-ray diffraction measurements were performed on the deterioration products scratched from the surface of cement paste. A Ricoh D/MAX-ⅢC X-ray diffraction machine was used in this study and the tube pressure was 35 kV with 30 mA using CoKα radiation. Data were collected between 2° and 70° (2θ) with a step-size of 0.02° at a speed of 8°/min.

The Fourier transform infrared spectra(FTIR) were recorded to assess the products from chemical reaction, where a Nicolet 5DXC Fourier transform infrared spectrometer ranging from 400 to 4 000 cm^{-1} was used.

3 Results and discussion

3.1 Visual inspection

A visual inspection was carried out at an interval of 60 days. The observations are summarized in Table 3. Typical photos of cube specimens stored in 5% $MgSO_4$ solution at 6 ℃ for 120 days and 240 days are showed in Fig.1 and Fig.2.

Table 2 Basic properties of cement

Normal consistency/%	Setting time/min		Soundness (Le chatelier test)	Flexural strength/MPa		Compressive strength/MPa	
	Initial setting	Final setting		3 d	28 d	3 d	28 d
25.0	108	180	Qualified	5.1	7.9	26.7	48.7

Table 3 Appearance change of cement paste samples

Samples	Exposed period/day			
	60	120	180	240
JY-1	No visible deterioration, white crystal	Some cracking at corners and along edges	Extensive cracking, slight spalling and hoary mush	Break up at corners and edges, severe spalling, and covered with a hoary mush
JY-2	No visible deterioration, white crystal	Some cracking at corners	Extensive cracking, expansion and slight spalling	Extensive cracking, expansion and spalling
JY-3	No visible deterioration, white crystal	No visible deterioration, white crystal	Cracking at corners, white crystal	Cracking at corners and edges, white crystal

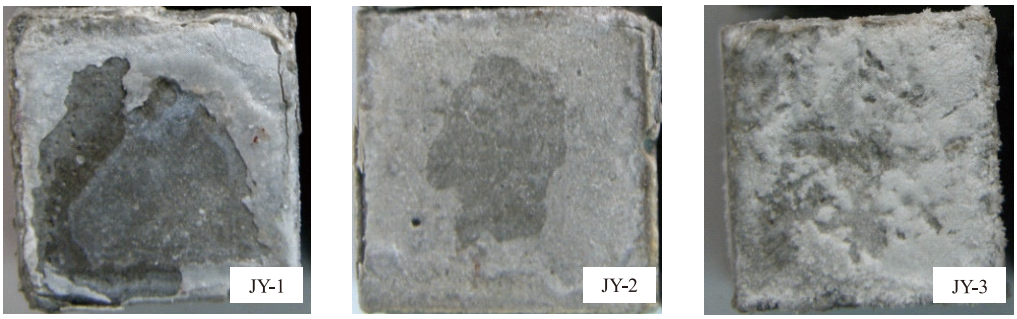

Fig.1 View of paste samples immersed in 5% $MgSO_4$ at 6 ℃ for 120 days

Fig.2 View of paste samples immersed in 5% $MgSO_4$ at 6 ℃ for 240 days

It can be found in Table 3 that except for white crystal on the surface, no other visible degradation occurred during the first 60 days for all specimens. The JY-1 (7 days water cured) showed the first signs of damage on the surface and edge after 120 days exposure. Sulfate attack was observed at the corners firstly followed by cracking along the edges and gradually extended to the surface of specimen combining with expansion and spalling. After 240 days exposure to the $MgSO_4$ solution, the surface of specimens was covered with a hoary mush, and beyond 2 mm from the surface no visible deterioration can be found.

As described in Table 3, sample with water curing of 28 days has exhibited advantage against sulfate attack at 6 ℃. Compared with JY-1, the deterioration intensity of JY-3 (28 days water cured) is significantly less at the same age, as well, the change of appearance is less obvious.

3.2 Compressive strength evolution

The results of compressive strength are shown in Fig.3. Two stages can be found. In the first stage, the compressive strength increases slowly as the exposed period increases. After exposure to the sulfate solution, the 90 days compressive strengths were 62.0, 66.3 and 64.3 MPa for JY-1, JY-2 (14 days water cured) and JY-3, respectively. These are partially associated with the improvement in the structure of cement paste due to topographic effects of limestone powder, and partially with respect to densifying pores for previous ingress and crystallization of sulfate ions[11]. In the second stage, the compressive strength decreases after 120 days due to serious sulfate attacks. At 240 days, the compressive strength of JY-1 specimens was only 31.9 MPa while the strength values of JY-2 and JY-3 specimens were 45.0 and 54.3 MPa, respectively. Powers and Brownyard reported that the hydration degree of Portland cement can reach 65% after 14 days curing, accompanied by a total pore ratio less than 20% of hardened paste[12]. Thus the resistance to sulfate attack in terms of strength loss greatly depends on curing time related to hydration process.

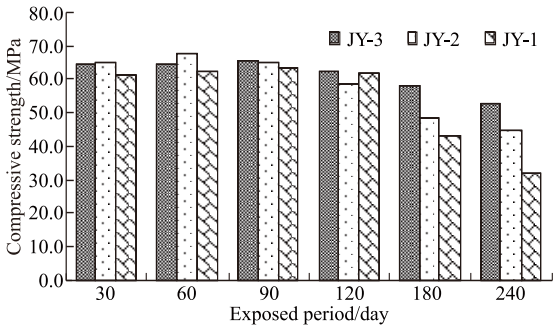

Fig.3 Compressive strength of paste specimens exposed to 5% $MgSO_4$ solution

3.3 Microstructure observations

XRD, FTIR and SEM-EDS measurements were carried out to identify the products of the sulfate attack. Cement paste samples were investigated by XRD after

240 days immersion in magnesium solution and the results are shown in Fig.4. The results indicate that the peaks of gypsum (d=7.630, 4.283, 3.065 Å) and calcite (d=3.033, 2.285, 1.874 Å) can be clearly detected in all samples, while the peak of JY-1 is the strongest among these three samples. The intensities of portlandite peaks were negligible in the XRD patterns as a result of reaction with magnesium sulfate to form gypsum and brucite. Compared with the three XRD patterns, the thaumasite formation with characteristic peaks (d=9.590, 3.801, 5.530 Å) appeared, which was in agreement with other studies[13,14]. As expected, it was found that the peak intensities of gypsum and ettringite (or thaumasite) increase with the curing time decreases.

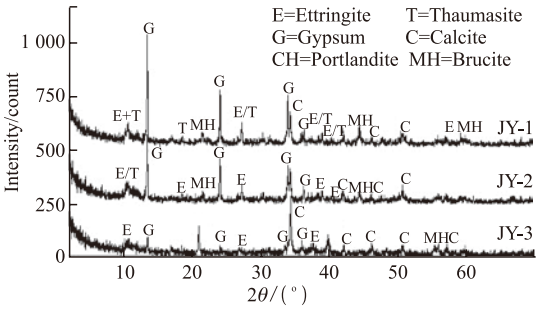

Fig.4 XRD patterns of degradation productions of paste samples for 240 days

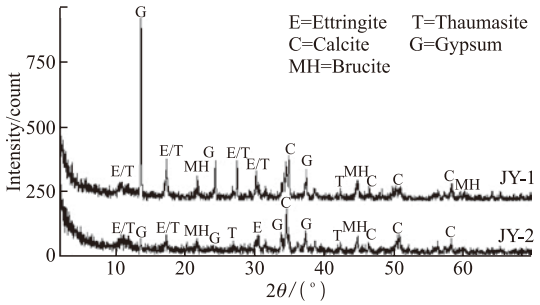

Fig.5 XRD patterns of fallen substance for 240 days

Fig.5 shows the XRD patterns of relevant fallen substance (from JY1 and JY2) at the bottom of the container after 240 days. Similar to Fig.4, there are obvious peaks corresponding to ettringite (thaumasite), gypsum, calcite as well as a lot of brucite, attributed to the reaction of Mg^{2+} from solution and OH^- dissolving from cement paste.

Considering the similar responses between thaumasite and ettringite (d=9.720, 5.610, 3.873 Å), further investigation was made using FTIR spectroscopy. The FTIR spectra taken from degradation productions of samples are shown in Fig.6. These three spectra are mostly similar except for small differences. For all samples, sharp bands at about 1 422 and 875 cm^{-1} were assigned to the appearance of $[CO_3]^{2-}$ groups. At the same time, the spectra showed the other strong band appearing at about 1 116 cm^{-1} that could be attributed to $[SO_4]^{2-}$ groups. For the exposure of 240 days, as expected, the maximal speak absorption of 669 cm^{-1} and the weak peak absorption of 499 cm^{-1} detected in the sample JY-1 are known to be the presence of $[SiO_6]^{2-}$ groups[15], which was the silica of octahedral arrangement.

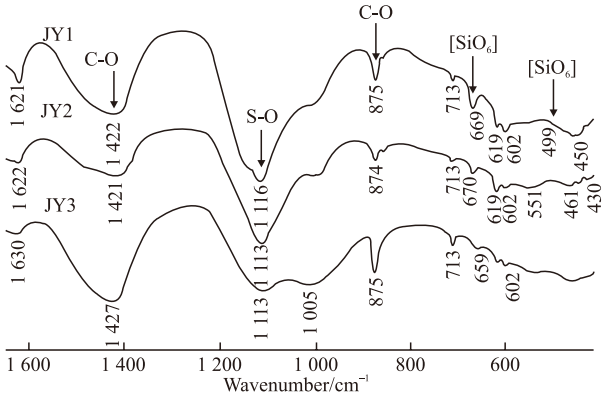

Fig.6 FTIR spectra of degradation productions of paste sample for 240 days (C-O—$[CO_3]^{2-}$, S-O—$[SO_4]^{2-}$)

Beyond the XRD and FTIR investigation, the SEM with an EDS profile from one point analysis was performed and the results are presented in Fig.7.

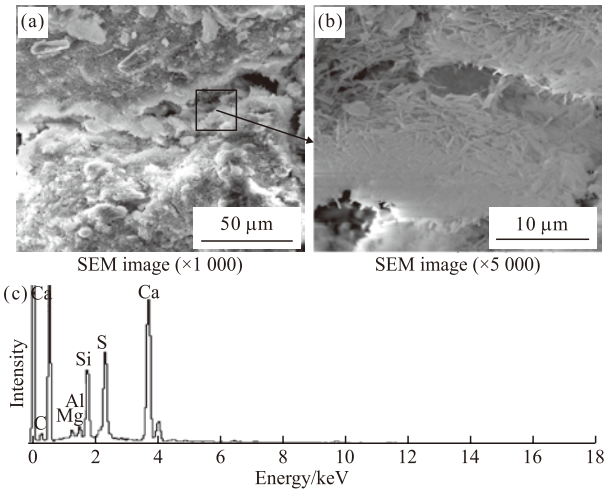

Fig.7 (a)(b)SEM images and (c)EDS profile (T) of cement paste sample for 240 days

Table 4 Content of the elements in the sample

Element	C	O	Mg	Al	Si	S	Ca	Total
Weight/%	4.14	59.56	0.66	0.96	5.81	7.34	21.53	100
Atomic/%	6.75	72.96	0.53	0.7	4.05	4.49	10.53	-

Fig.7 shows two magnifications, clearly illustrating that the cement specimens were partially replaced by limestone powder suffered from sulfate

attack accompanied by great straight, smooth and feather-like crystals of lengths mainly ranging between 3 and 5 μm in large zone, as reported elsewhere[16]. According to Sahu and Badger[17], the characteristic peaks of thaumasite crystal were Ca, S and Si in EDS spectrum, while the characteristic peaks of ettringite crystal were Ca, S and Al in EDS spectrum. The EDS profile of the needle-shaped crystals indicates the presence of Ca, Si, S and O, whereas no signal of Al was found, confirming the presence of thaumasite. As shown in Table 4, the analysis of the compositions seems to yield the elements distribution close to that of thaumasite (Ca:Si:S=3:1:1[18] by molar). Therefore, it suggests that the samples water curing duration has a significant effect on TSA.

4 Conclusions

a) Cement pastes incorporated with 30% limestone powder were found to be susceptible to the thaumasite form of sulfate attack after exposure to a 5% magnesium sulfate at 6 ℃. Along with ettringite and gypsum, thaumasite was detected in the cement paste for 240 days storage. The intensity of deteriorations was greater and earlier with shortening of the curing time prior to the exposure to the sulfate solution.

b) Extensive deteriorations in terms of a white, mushy, and incohesive matrix due to the formation of thaumasite were observed, especially in the samples water-cured for 7 days. The damage occurred on the surface of the cement paste specimens firstly, and then proceeded inwards.

c) With respect to permeation and crystallization of sulfate ions, and topographic effect of limestone power, the compressive strength of cement specimens increased slowly and subsequently decreased due to sulfate attack after an exposure for 120 days.

References

[1] Collepardi M. Thaumasite Formation and Deteriorarion of Historical Buildings[J]. *Cement and Concrete Composites*, 1999, 21: 147-154

[2] S Kohler, Heinz D, Urbonas L. Effect of Etringite on Thaumasite Formation[J]. *Cement and Concrete Research*, 2006, 36: 697-706

[3] Crammond N J. Thaumasite in Failed Cement Mortars and Renders from Exposed Brickwork[J]. *Cement and Concrete Research*, 1985, 15: 1 039-1 050

[4] Romer M. Steam Locomotive Soot and the Formation of Thaumasite in Shotcrete[J]. *Cement and Concrete Composites*, 2003, 25: 147-154

[5] Erlin B, Stark D C. Identification and Occurrence of Thaumasite in Concrete[J]. *Highway Research Record*, 1965, 113: 108-113

[6] Crammond N J, Norah C. The Occurrence of Thaumasite in Modern Construction-a Review[J]. *Cement and Concrete Composites*, 2002, 24: 393-402

[7] Santhanam M, Cohen M D, Olek J. Mechanism of Sulfate Attack: A Fresh Look Part 1:Summary of Experimental Resuns[J]. *Cement and Concrete Research*, 2002, 32: 915-921

[8] Crammond N J. The Thaumasite Form of Sulfateattack in the UK[J]. *Cement and Concrete Composites*, 2003, 25: 809-818

[9] Hartshorn S A, Sharp J H, Swamy R N. Thaumasite Formation in Portand-limestone Cement Pastes[J]. *Cement and Concrete Research*, 1999, 29: 1 331-1 340

[10] Hui Y, Bin X X, Liu B W, *et al.* Effect of Initial Curing Conditions on Thaumasite Form of Sulfate Attack of Cement Based Materials[J]. *Applied Mechanics and Materials*, 2013, 275-277: 2 136-2 140

[11] Hansen T C. Physical Structure of Harden Cement Paste[J]. *A Classical Approach, Materials and Structures*, 1986, 19: 423-436

[12] Powers T C, Brownyard T L. Studies of the Physical Properties of Hardened Portland Cement Paste[J]. *Journal of American Concrete Institute*, 2003, 25(8): 59-70

[13] Edge R A, Tayler H FW. Crystal Structure of Thaumasite, $[Ca_3Si(OH)_6 \cdot 12H_2O](SO_4)(CO_3)$ [J]. *Acta Crystallographica: Section B*, 1971, 27: 594-601

[14] Bensted J. Some Problems with Ettringite and Thaumasite in the Gypsum Plaster/Cement Contact Area[C]. *Proceedings of the International RILEM Symposium on Calcium Sulfates and Derived Materials*, France, 1977

[15] Lachowski E E, Barnett S J, Macphee D E. Transmission Electron Optical Study of Ettringite and Thaumasite[J]. *Cement and Concrete Composites*, 2003, 25: 819-822

[16] Torres S M, Lynsdale C J, Swamy R N, *et al*. Microstructure of 5-year-old Mortars Containing Limestone Filler Damaged by Thaumasite[J]. *Cement and Concrete Research*, 2006, 36: 384-394

[17] Sahu S, Badger S. Evidence of Thaumasite Formation in Southern California Concrete[J]. *Cement and Concrete Composites*, 2002, 24: 379-384

[18] Justnes H. Thaumasite Formed by Sulfate Attack on Mortar with Limestone Filler[J]. *Cement and Concrete Composites*, 2003, 25: 955-959